

Data-driven Modelling of Prognostics of Lithium-ion Batteries Using LSTM

Shreya Shinde¹, Lennard Dsouza¹, Snehal Maria¹, Shivam Anvekar¹, Abhishek Shiwalkar²

¹Student, Department of Electrical Engineering, Fr. C. Rodrigues Institute of Technology, Vashi, Navi Mumbai, Maharashtra, India

²Professor, Department of Electrical Engineering, Fr. C. Rodrigues Institute of Technology, Vashi, Navi Mumbai, Maharashtra, India

Abstract - The rechargeable lithium-ion battery has been extensively used in mobile communication and portable instruments due to its many advantages, such as high volumetric and gravimetric energy density and low self-discharge rate. Early detection of inadequate performance facilitates the timely maintenance of battery systems. This reduces operational costs and prevents accidents and malfunctions. Prognostic and health management (PHM) can ensure that a lithium-ion battery is working safely and reliably. The main approach of the PHM evaluation of the battery is to determine the state of health (SoH) and state of charge (SOC) of the battery. This paper presents the preliminary development of the data-driven prognostic, using an LSTM (RNN) approach to predict the SoH and SoC of the lithium-ion battery. The effectiveness of the proposed approach was assessed in a case study using a battery dataset from NASA's Ames Prognostics Center of Excellence (PCoE) database. The proposed LSTM algorithm was compared against other machine learning based on the RMSE value. The experimental results reveal that the performance of the LSTM algorithm could either match or outweigh other machine learning algorithms.

Key Words: lithium-ion battery, battery management system, Prognostic and health management, State of Health, State of Charge, LSTM

1. INTRODUCTION

Li-ion batteries are playing a crucial role in the fields of renewable energy systems and electric vehicles. Batteries hold the potential to transform the transportation sector, which now emits considerable volumes of CO₂. They also provide a solution to the intermittent energy powered by solar and wind generators, assisting in the viability of these green solutions. However, batteries may not be the clean energy solution they seem at face value. Obtaining resources for batteries, such as lithium, has become an environmental issue[1]. The reliability of these systems depends on a battery management system (BMS) which monitors the state of charge (SoC) and state of health (SoH) effectively[2]. Knowing the SoH of a battery in advance enhances the system's reliability. The proposed SoH estimation method is simulated in Python using the LSTM algorithm by

considering the ageing factors such as temperature, charge/discharge rates, and depth of discharge[3].

2. SOC AND SOH ESTIMATION

Due to the restricted manufacturing process, the actual full capacity of a new battery may differ from the nominal battery capacity claimed by the manufacturer. As a result, a new battery's original maximum capacity, Q_f , is calculated by averaging the full capacities of multiple charging/discharging cycles. When a battery begins a cyclic charging/discharging operation, the inevitable aging will lead to performance deterioration, with a decrease in the maximum chargeable or releasable capacity, Q_M , which is acquired by cumulating the battery charges either from an empty-to-full or full-to-empty operation[5]. The "state of health" of a battery describes the difference between an examined battery and a new battery, taking into account cell ageing. It's the ratio of a battery's maximum charge to its rated capacity[6].

$$SoH(\%) = 100 \frac{Q_{maximum}}{C_{rated}}$$

For an aged battery, the capacity fading causes not only a decrease in the maximum releasable capacity but also a mistake in SOC estimation. The state of charge of a battery describes the difference between a fully charged battery and the same battery in use. It is associated with the remaining quantity of electricity available in the cell[6]. It is calculated by dividing the battery's remaining charge by the maximum charge the battery can produce.

$$SoC(\%) = SoC_o(\%) + 100 \frac{Q_o + Q}{Q_{max}}$$

3. DATA SET

The lithium-ion battery data employed in the prognostics analysis of this work was retrieved from the NASA Ames Prognostics Center of Excellence (PCoE) data repository[4]. This dataset contains the test results of commercially available lithium-ion 1850-sized rechargeable batteries, and the experiments have been performed under controlled

conditions in the NASA prognostics testbed. The dataset contains the test results of commercially available lithium-ion 1850-sized rechargeable batteries. A set of four Li-ion batteries (# 5, 6, 7, and 18) were run through three different operational profiles (charge, discharge, and impedance) at room temperature. Charging was carried out in a constant current (CC) mode at 1.5A until the battery voltage reached 4.2V and then continued in a constant voltage (CV) mode until the charge current dropped to 20mA. Discharge was carried out at a constant current (CC) level of 2A until the battery voltage fell to 2.7V, 2.5V, 2.2V, and 2.5V for batteries 5, 6, 7, and 18 respectively. Impedance measurement was carried out through an electrochemical impedance spectroscopy (EIS) frequency sweep from 0.1Hz to 5kHz. Repeated charge and discharge cycles result in accelerated ageing of the batteries, while impedance measurements provide insight into the internal battery parameters that change as ageing progresses. The experiments were stopped when the batteries reached end-of-life (EOL) criteria, which was a 30% fade in rated capacity (from 2Ahr to 1.4Ahr). The various parameters in the data set consist of charge, discharge, and impedance fields.

3.1 Data Analysis

The following data set was parsed in Python 3.9 using the SciPy library and the following characteristics were observed during charge and discharge of Battery no.5 across a total of 164 cycles. Graphs were plotted at intervals of 30 cycles to get a clear idea of the distinct nature of the characteristics with the passing cycles.

3.1.1 Charging Characteristics

Charging was carried out in a constant current (CC) mode at 1.5A until the battery voltage reached 4.2V, which is the threshold voltage, and then continued in a constant voltage (CV) mode until the charge current dropped to 20mA. The voltage measured across the battery increases slowly in each cycle. However, because the battery cannot maintain its initial voltage value with each cycle, we observe a variation in the starting level of the voltage (as after one complete cycle of discharge, some amount of energy is stored within the battery). The charging voltage is slightly greater than the current measured due to some drop assumed. The amount of time taken for fully charging the battery is a specific time (1 hr) after the battery enters the CV mode of charging, usually when the current reaches 10 percent

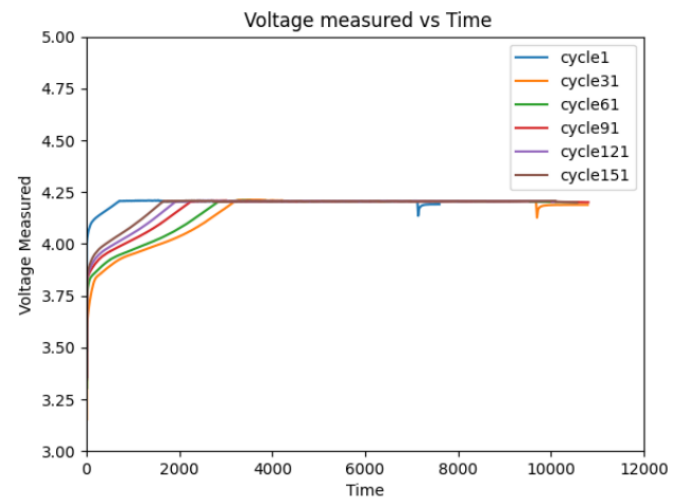


Chart -1: Voltage measured Vs Time while charging (Battery No. 5)

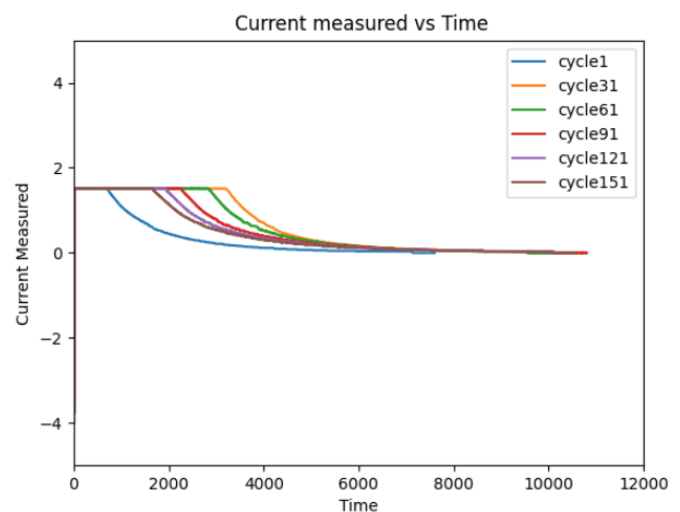


Chart -2: Current measured Vs Time while charging (Battery No. 5)

3.1.2 Discharging Characteristics

The battery was discharged at a constant current (CC) of 2A until the voltage dropped to 2.7V. Since the battery's capacity is 1.9Ahr, the battery is discharged at 1.1C in this situation. In the graphs shown below, we observe that with the passing of cycles, the rate of discharge increases, suggesting that the cut-off voltage is reached sooner, which is an indication that the battery is getting older. Once the cut-off voltage is reached, the battery cannot be discharged any further as it's critical for the battery's longevity. Discharging of a battery takes place when the battery is connected across the load. The voltage across the load is slightly less due to the drop across the circuit and battery back emf with a constant current of 2A applied throughout.

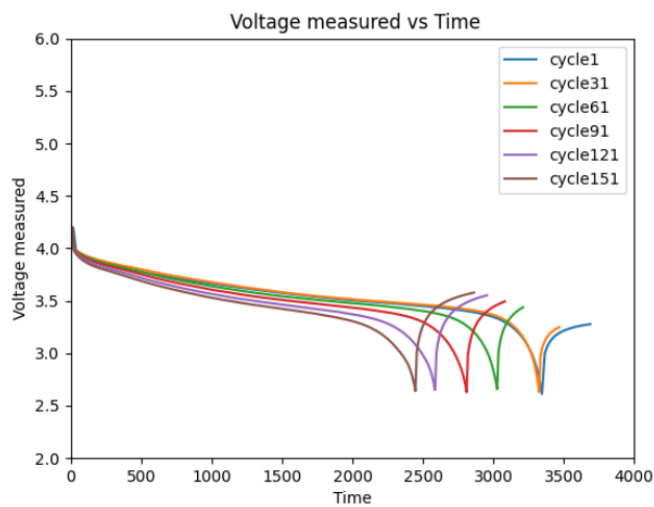


Chart -3: Measured measured Vs Time while discharging (Battery No. 5)

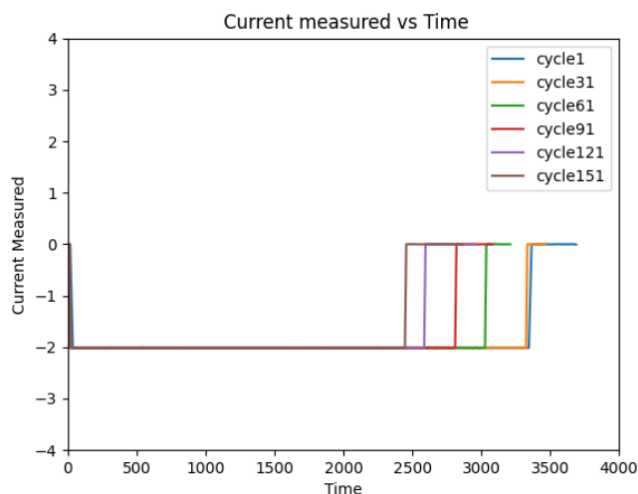


Chart -4: Current measured Vs Time while discharging (Battery No. 5)

current dropped to 19mA. Discharge was carried out at a constant current (CC) level of 1A until the battery voltage fell to 2.7V, 2.5V, 2.2V, and 2.5V for the battery[8]. The current sensor is always in series with the battery. Therefore, a close resemblance was observed between the practically performed data and the theoretically observed data in the datasheet mentioned in our chosen research paper. The data was acquired by connecting the chassis to the LabVIEW using the laptop interface. An electronic load was used to carry out the discharging of the battery, and probes from NI modules across the battery were connected to measure the voltage. A current sensor was connected in series to the battery to measure the current and was calibrated using the Arduino Uno. A K-Type Thermocouple was placed over the battery with the help of insulation tape for accurate measurement of the battery temperature[9]. For charging, a calibrated charger was dismantled and the phase and neutral terminals were directly inserted into the supply charging slots. Data for charging or discharging cycles was continuously monitored in the LabVIEW at a frequency of 1 Hz until the end of the cycle. The challenges faced while executing the hardware were that the LabVIEW could only acquire data from one NI-Module at a time, which led to us performing different cycles for the measurement of voltage and temperature for their respective NI-Modules to get the readings for a single cycle[10]. The data was acquired and proved to be authentic as it followed the ideal (theoretical) charging and discharging traits.



Fig -1: Hardware setup for generating real-time data

4. HARDWARE IMPLEMENTATION

Assembly of hardware equipment was initially problematic because to the COVID-19 outbreak, but once the college reopened, hardware was installed to validate the data obtained from our study paper, which we referred to for benchmark results. This was achieved by charging and discharging 18650 Li-ion batteries with identical specifications (nominal voltage 3.7V, peak voltage 4.2V, ampere-hour capacity 2000mAh) using LabVIEW software and NI-Modules.

4.1 Working

Charging was carried out in a constant current (CC) mode at 1.3A until the battery voltage reached 4V and then continued in a constant voltage (CV) mode until the charge

4.2 Block Diagram

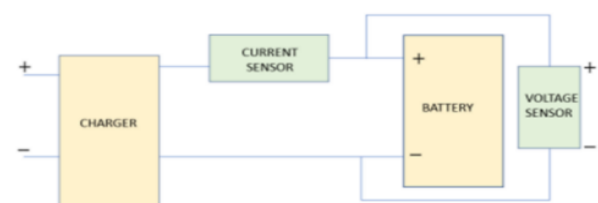


Fig -2: block diagram for charging cycle

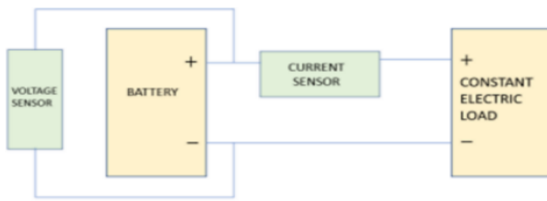
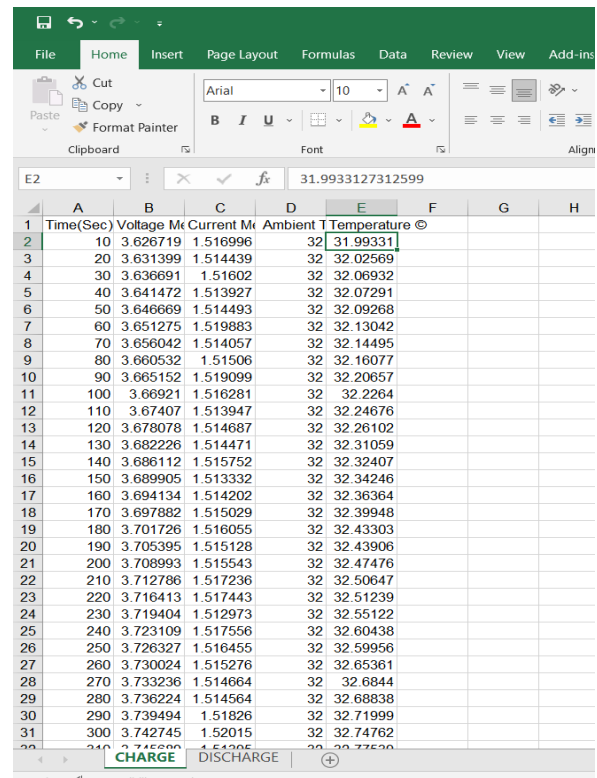


Fig -3: Block diagram for discharging cycle

4.3 Result

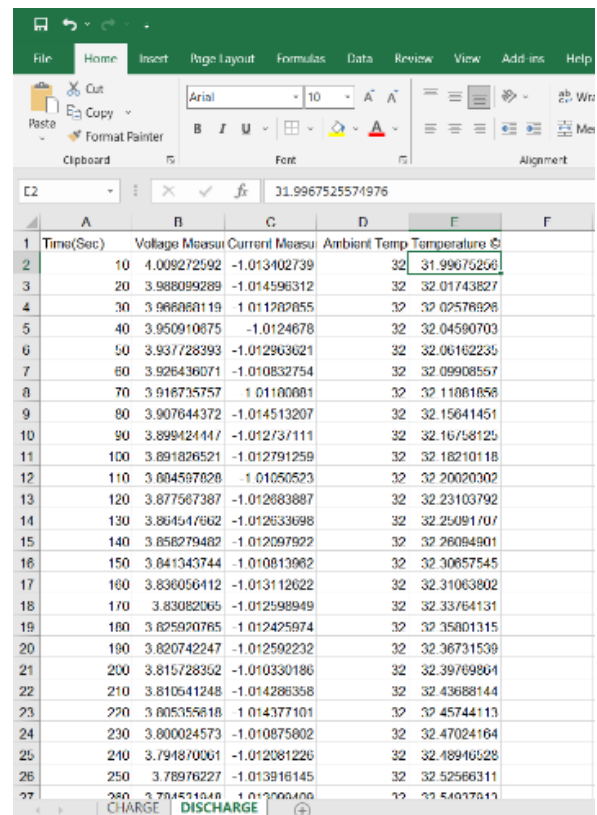
The following parameters were captured during the charging and discharging of the batteries,

- i. The voltage rose from the nominal voltage of 3.7V to 4V, 4.1V during charging, and then fell to 2.7V, which was the cut-off voltage during discharging.
- ii. The current was drawn using a constant electronic load of 1A during discharging at 0.5C. While charging, it follows the CC-CV protocols where first the charging takes place at a constant current of 1.3A till the voltage rises from the nominal voltage of 3.7V to 4.2V, after which the current starts to fall, till it reaches 50 milliamps.
- iii. The temperature at which the entire setup was being performed was 32°C room temperature or ambient temperature. We observed that with the rise of current, the temperature gradually rose from 32°C to a small amount of 34°C at its peak current and then the temperature subsided gradually. But the temperature rise during discharging was rapid as a constant current of 1 ampere was being absorbed by the load continuously, which led to a rise in temperature to 36°C.



Time (Sec)	Voltage Meas	Current Meas	Ambient Temp	Temperature
10	3.626719	1.516996	32	31.99331
20	3.631399	1.514439	32	32.02569
30	3.636691	1.516002	32	32.06932
40	3.641472	1.513927	32	32.07291
50	3.646669	1.514493	32	32.09268
60	3.651275	1.519883	32	32.13042
70	3.656042	1.514057	32	32.14495
80	3.660532	1.515006	32	32.16077
90	3.665152	1.519099	32	32.20657
100	3.66921	1.516281	32	32.2264
110	3.67407	1.513947	32	32.24676
120	3.678078	1.514687	32	32.26102
130	3.682226	1.514471	32	32.31059
140	3.686112	1.515752	32	32.32407
150	3.689905	1.513332	32	32.34246
160	3.694134	1.514202	32	32.36364
170	3.697882	1.515029	32	32.39948
180	3.701726	1.516055	32	32.43303
190	3.705395	1.515128	32	32.43906
200	3.708993	1.515543	32	32.47476
210	3.712786	1.517236	32	32.50647
220	3.716413	1.517443	32	32.51239
230	3.719404	1.512973	32	32.55122
240	3.723109	1.517556	32	32.60438
250	3.726327	1.516455	32	32.59956
260	3.730024	1.515276	32	32.65361
270	3.733236	1.514664	32	32.6844
280	3.736224	1.514564	32	32.68838
290	3.739494	1.51826	32	32.71999
300	3.742745	1.52015	32	32.74762

Fig -4: Data acquisition of charging Setup



Time (Sec)	Voltage Meas	Current Meas	Ambient Temp	Temperature
10	4.009272592	-1.013402739	32	31.99675266
20	3.988099289	-1.014596312	32	32.01743827
30	3.966868119	-1.011282855	32	32.02576828
40	3.950910875	-1.0124678	32	32.04590703
50	3.937728393	-1.01293621	32	32.06162235
60	3.926436071	-1.010832754	32	32.09908557
70	3.916735757	-1.01100081	32	32.11861858
80	3.907644372	-1.014513207	32	32.15641451
90	3.899424447	-1.012737111	32	32.16758125
100	3.891826521	-1.012791259	32	32.18210118
110	3.884587828	-1.01050523	32	32.20020302
120	3.877567387	-1.012883887	32	32.23103792
130	3.864547662	-1.012633698	32	32.25091707
140	3.858279482	-1.012097922	32	32.26084901
150	3.841343744	-1.010813082	32	32.30857545
160	3.830056412	-1.013112622	32	32.31063802
170	3.83082065	-1.012598949	32	32.33764131
180	3.825920785	-1.012425974	32	32.35801315
190	3.820742247	-1.012592232	32	32.36731539
200	3.815728352	-1.010330186	32	32.39769804
210	3.810541248	-1.014286358	32	32.43688144
220	3.805355818	-1.014377101	32	32.45744113
230	3.800024573	-1.010875802	32	32.47024164
240	3.794870061	-1.012081226	32	32.48940528
250	3.78976227	-1.013916145	32	32.52566311
260	3.78451548	-1.01390406	32	32.54078811

Fig -5: Data acquisition of discharging Setup

5. MACHINE LEARNING ALGORITHMS

Machine learning algorithms are good at handling data that is multidimensional and multivariate, and they can do this in dynamic or uncertain environments. As ML algorithms gain experience, they keep improving in accuracy and efficiency. This lets them make better decisions. Say you need to make a weather forecast model. As the amount of data, you have keeps growing, your algorithms learn to make more accurate predictions faster [7]. There is a lot of scope in ML to become the top technology in the future[4]. The reason is that it has a lot of research areas in it. This helps us improve both hardware and software.

5.1 Proposed ML algorithm LSTM

Long Short-Term Memory networks – usually just called “LSTMs” – are a special kind of Recurrent Neural Network, Capable of learning long-term dependencies. They were introduced by Hochreiter Schmidhuber (1997) and were refined and popularized by many people. They work tremendously well on a large variety of problems and are now widely used[11].

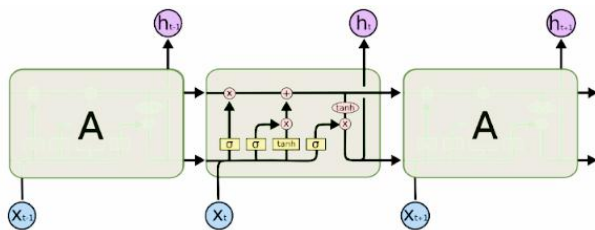


Fig -6: LSTM block diagram

Recurrent networks can, in principle, use their feedback connections to store representations of recent input events in the form of activations (weights). This is potentially significant for many applications, including speech processing, non-Markovian control, and music composition. Although theoretically fascinating, existing methods do not provide clear practical advantages over backdrops in feedforward nets with limited time. With conventional “Back-Propagation Through Time” or “Real-Time Recurrent Learning”, error signals flowing backwards in time tend to either (1) blow up or (2) vanish the temporary backpropagated error. This may affect the model and bring about the following consequences: Case (1) may lead to oscillating weights. Case (2): Learning to bridge long time lags takes a prohibitive amount of time or does not work at all. In conjunction with an appropriate gradient-based learning algorithm, this paper presents “Long Short-Term Memory” (LSTM), a novel recurrent network architecture in conjunction with an appropriate gradient-based learning algorithm. LSTM is designed to overcome these error back-flow problems. It can learn to bridge time intervals over 1000 steps, even in the case of noisy, incompressible input sequences, without loss of short time lag capabilities. This is

achieved by an efficient, gradient-based algorithm. LSTM outperforms and also learns to solve complex, artificial tasks no other recurrent algorithm has solved before. The other advantages of using LSTM are as follows: - For long time lag problems, LSTM can handle noisy distributed representations and continuous values. In contrast to finite-state automata or hidden Markov models, LSTM does not require an a priori choice of a finite number of states. In principle, it can deal with unlimited state numbers. There appears to be no need for parameter fine-tuning. LSTM works well over a broad range of parameters such as learning rate, input gate bias, and output gate bias. Positions of widely separated, relevant inputs in the input sequence do not matter. The LSTM algorithm updates complexity per weight and time step [12]. LSTM is local in both space and time.

$$MSE = \frac{1}{K} \sum_{k=1}^k (y_k - y_k')^2$$

$$RMSE = \sqrt{\frac{1}{K} \sum_{k=1}^k (y_k - y_k')^2}$$

5.2 Reason for not Implementing SoC Estimation

Precise measurements of SOC are necessary to ensure safe operation while maximizing the use of battery capacity. In early applications, people found that the battery SOC had a strong linear relationship with the open-circuit voltage (OCV). To measure the accurate OCV, the battery needs hours to rest. While in most conditions, accurate OCV is unlikely to be obtained and is mainly not a method considered in the case of finding a soc for lithium-ion batteries. Due to the various internal and external conditions, fixed mathematical transformations cannot be accurate. The coulomb counting method (CCM) is another straightforward method that has the advantage of simple computation and easy implementation. CCM is widely recommended for battery health management. However, CCM is calculated by charge and discharge current time integral, which is unable to eliminate cumulative error and is very sensitive to the initial value. If the initial SOC value is inaccurate, it will affect all estimates and the error will accumulate during the whole estimation process. The initial SoC value is usually predicted and is not verified to be 100% accurate. The large amount of data makes it even more difficult for the model to give an accurate SOC value[14].

6. SOH MODELLING USING LSTM

In this section, an analysis of battery No. 06, No. 07, and No. 18 degradation datasets taken from the NASA Ames Prognostics Center of Excellence (PCoE) database was conducted to evaluate the effectiveness of the developed LSTM technique. The dataset of battery No. 05 was employed

as a training dataset. A detailed description of the experimental data has been provided. The SoH experimental results from the conventional DNN and developed LSTM model will be presented. An LSTM-RNN network is trained to model the complex battery dynamics under varying ambient temperatures. A step-by-step searching method is presented to determine the optimal network hyper-parameters for SOH modelling[13]. The network well learns the battery dynamics, presents good robustness against unknown initial states and provides satisfying SOH estimations under varying temperatures. There are natural recursive linkages between current SOC and past inputs, as illustrated by the Coulomb counting approach. An LSTM-RNN network is therefore constructed to model the temporal dependencies of the input layer, battery current, terminal voltage, and ambient temperature to form the input vector. Since it is necessary to calculate the SoH of the battery, as this is the data that will be predicted using the LSTM model, a theoretical calculation of SOH was performed in Python based on the formula given below:

$$SoH(\%) = 100 \frac{Q_{maximum}}{C_{rated}}$$

- where,

$Q_{maximum}$ represents the maximum practical capacity as measured from the operating battery at the current time.

C_{rated} represents the rated capacity from battery manufacturers. Theoretical value of SoH of all the batteries was calculated and plotted in the graph showing the aging process of the battery[15].

According to the README file of the dataset, the data is stored in several ".mat" files. Each file corresponds to a specific battery, and the data structure of each file contains the parameters mentioned in the above section. For the LSTM model proposed in Section V, it is only necessary to collect the data related to the discharge of the battery. For this, a function is created in Python that is in charge of reading this data from the ".mat" file and storing it in memory in two pandas Data Frames for later access. After loading the dataset, a description of the data is made using pandas functions to verify if the data loading was correct.

	cycle	datetime	capacity	SoH
0	1	2008-04-02 15:25:41	2.035338	1.000000
1	2	2008-04-02 19:43:48	2.025140	0.994990
2	3	2008-04-03 00:01:06	2.013326	0.989185
3	4	2008-04-03 04:16:37	2.013285	0.989165
4	5	2008-04-03 08:33:25	2.000528	0.982898
...
163	164	2008-05-26 10:44:38	1.153818	0.566893
164	165	2008-05-26 15:30:43	1.164401	0.572092
165	166	2008-05-26 20:21:04	1.158797	0.569339
166	167	2008-05-27 15:52:41	1.174975	0.577287
167	168	2008-05-27 20:45:42	1.185675	0.582545

Fig -7: Dataset after formatting and parsing

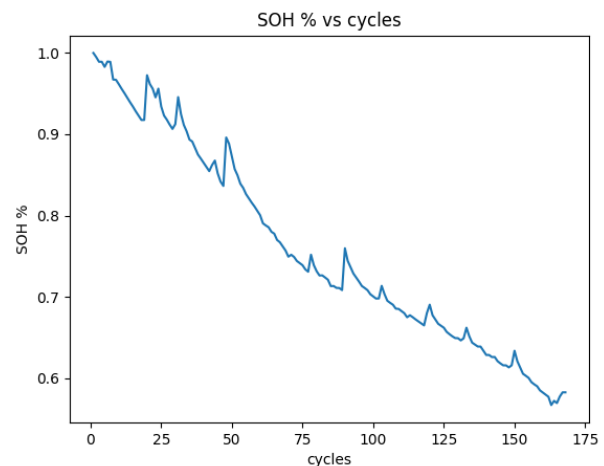


Chart -5: Actual SoH vs cycles

6.1 Training phase for calculating SoH

The dataset is prepared in such a way that it can be used by TensorFlow during the training phase; two structures are constructed corresponding to the predicted input and output. For the input data, the relevant characteristics of the dataset are filtered, which are:

- Battery capacity
- Voltage
- Current
- Temperature
- Charging voltage
- Charging current
- Instant of time (from the start of the download)

For the output data, the SoH of the battery is calculated and, in both input and output cases, the values are normalized to a range of values between [0] and [1]. For the preparation of the model, four dropout layers, one dense layer, and one of the ADAM types are used as optimizers. About 50 epochs are used for training the model.

Layer (type)	Output Shape	Param #
lstm_12 (LSTM)	(None, 7, 200)	161600
dropout_16 (Dropout)	(None, 7, 200)	0
lstm_13 (LSTM)	(None, 7, 200)	320800
dropout_17 (Dropout)	(None, 7, 200)	0
lstm_14 (LSTM)	(None, 7, 200)	320800
dropout_18 (Dropout)	(None, 7, 200)	0
lstm_15 (LSTM)	(None, 200)	320800
dropout_19 (Dropout)	(None, 200)	0
dense_19 (Dense)	(None, 1)	201

 Total params: 1,124,201
 Trainable params: 1,124,201
 Non-trainable params: 0

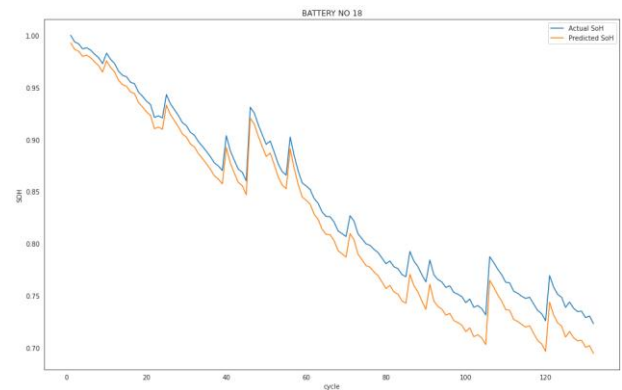


Chart -8: Battery No. 18

Fig -8: LSTM model created from training data-set

6.2 Testing to check the correctness of the model

The information (or data) of the test batteries, namely Battery No. 6, Battery No. 7, and Battery No. 18, was loaded to test the model's correctness. The root of the mean square error, as well as the true SoH and the SoH predicted by the network, were calculated in a table. In addition, a plot of cycles vs. SoH for each of the three batteries was created.

6.3 Result

In this experiment, the discharge data for all 164 cycles from battery No. 5 were employed. The SoH was calculated from the initial capacity as being 1.9 Ahr. The result is considered to be a long-term SoH estimation of the battery. The following graphs show the performance of battery no. 6, 7, and 18 using a complex DNN algorithm (LSTM). The x-axis represents the cycles, and the y-axis represents the SoH. The blue line in the plot represents the actual SoH and the orange line represents the predicted SoH by the model.

It is clearly shown in the figures that due to the accurate fitting of the trained DNN model with batteries no. 6, 7 and 18, the LSTM model is successfully built and the RMSE of the SoH estimated by the proposed model is much less as compared to other traditional machine learning algorithms.

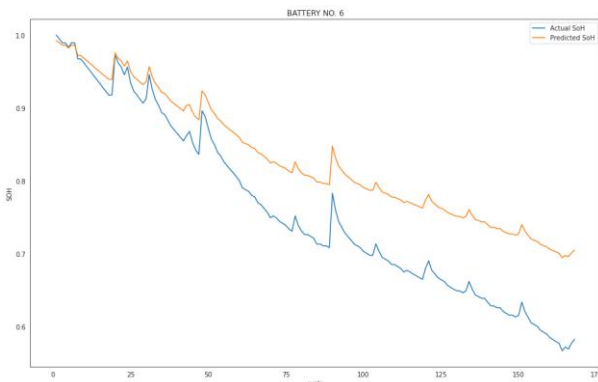


Chart -6: Battery No. 6

Table -1: RMSE of the SoH estimation by using LSTM and traditional machine learning algorithms

RMSE					
K-NN	LR	SVM	ANN	DNN	LSTM
5.598	4.558	4.552	4.611	3.427	2.406

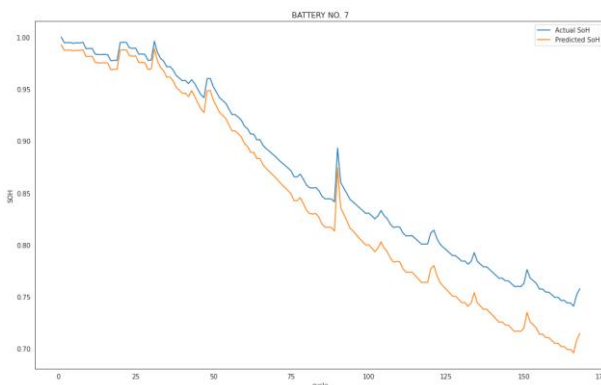


Chart -7: Battery No. 7

Considering the results illustrated above, it is also important to note that the results from battery No. 06 performed slightly worse when compared to battery No. 07 and 18. This could be due to the ageing pattern of battery No. 06 being slightly different from the training dataset.

Furthermore, as compared to the other batteries, the results for battery No. 06 had a wider distribution. The results from the table given below show that, overall, the proposed LSTM algorithm outperformed all the traditional machine learning algorithms, including the standard DNN method. LSTM performed better, in terms of capturing the RMSE value.

Absolute errors measured the mean absolute value of the difference between the elementwise inputs. The absolute error formula used as the loss function can be expressed by the following equation:

$$\text{Absolute Error Loss} = \frac{1}{K} |y_k - \hat{y}_k|^2$$

Where, y_i and \hat{y}_i are, respectively, the predicted data and the input data of each iteration or epoch i , and k is the number of iterations or epochs. In this experiment, the total number of epochs was set to 200.

7. CONCLUSIONS

This work aims to develop an LSTM model to predict the state of health of lithium-ion batteries. This experiment has achieved its goal of aiding, as a benchmark, the prognostic data-driven model for battery data using machine learning algorithms. Based on the results from the case studies, it shows that the LSTM algorithm provides a promising outcome for predicting and modelling prognostic data, especially in the battery prognostic and health management applications. Also, based on several advantages of data-driven models over the traditional physics-based models and the accuracy achieved, we believe that the traditional physics-based model may be replaced by data-driven models soon, in various fields and applications. This future trend of data-driven models is in line with the recent achievement of deep learning algorithms and artificial intelligence. These methodologies are believed to be the main approaches in the further development of data-driven models. However, the accuracy of prediction and the higher performance of using deep learning algorithms also come with the drawback of higher computational time. With rapid advancements in technology, the computational time could be substantially reduced. The future direction of this work will focus on developing a hybrid-deep learning model that could be universally applicable to multiple types of prognostic data. Due to time constraints and inaccessibility of the lab equipment, it was not feasible to create an entire dataset of the battery as acquiring an entire dataset would take approximately $(170 \times 4) = 680$ hours. Hence, there is uncertainty in predicting the whole nature of the battery's operation based on a couple of charge-discharge cycles. However, it was found that in the practically performed cycles, all the charging/discharging protocols were observed quite accurately.

ACKNOWLEDGEMENT

The success of a project like this, involving high technical expertise, patience, and the massive support of guides, is possible when team members work together. We take this opportunity to express our gratitude to those who have been instrumental in the successful completion of this project. We

would like to show our appreciation to Mr Abhishek Shiwalkar and Dr Sushil S. Thale for their guidance and support, which was instrumental in the progress of this project. We would also like to thank our project coordinator, Mrs Seema Jadhav for providing us with regular input about documentation and the project timeline. We would also like to thank Mr Nikhil Sorade for his guidance and support in data set interpretation. A big thanks to our HOD, Dr Bindu S. for all the encouragement given to our team. We would also like to thank our principal, Dr S. M. Khot for giving us the opportunity and the environment to learn and grow.

REFERENCES

- [1] H. C. Hesse, M. Schimpe, D. Kucevic, and A. Jossen, "Lithium-ion battery storage for the grid—a review of stationary battery storage system design tailored for applications in modern power grids," *Energies*, vol. 10, no. 12, p. 2107, 2017.
- [2] R. Xiong, Y. Zhang, J. Wang, H. He, S. Peng, and M. Pecht, "Lithium-ion battery health prognosis based on a real battery management system used in electric vehicles," *IEEE Transactions on Vehicular Technology*, vol. 68, no. 5, pp. 4110–4121, 2018.
- [3] J. Duan, X. Tang, H. Dai, Y. Yang, W. Wu, X. Wei, and Y. Huang, "Building safe lithium-ion batteries for electric vehicles: a review," *Electrochemical Energy Reviews*, vol. 3, no. 1, pp. 1–42, 2020.
- [4] P. Khumprom and N. Yodo, "A data-driven predictive prognostic model for lithium-ion batteries based on a deep learning algorithm," *Energies*, vol. 12, no. 4, p. 660, 2019.
- [5] J. Vetter, P. Novák, M. R. Wagner, C. Veit, K.-C. Moller, J. Besenhard, M. Winter, M. Wohlfahrt-Mehrens, C. Vogler, and A. Hammouche, "Ageing mechanisms in lithium-ion batteries," *Journal of power sources*, vol. 147, no. 1-2, pp. 269–281, 2005.
- [6] S.-C. Huang, K.-H. Tseng, J.-W. Liang, C.-L. Chang, and M. G. Pecht, "An online soc and soh estimation model for lithium-ion batteries," *Energies*, vol. 10, no. 4, p. 512, 2017.
- [7] J. S. Goud, R. Kalpana, and B. Singh, "An online method of estimating state of health of a li-ion battery," *IEEE Transactions on Energy Conversion*, vol. 36, no. 1, pp. 111–119, 2020.
- [8] P. Ferrand, "Gpscan. vi: A general-purpose labview program for scanning imaging or any application requiring synchronous analog voltage generation and data acquisition," *Computer Physics Communications*, vol. 192, pp. 342– 347, 2015.

- [9] S. A. Hasib, S. Islam, R. K. Chakraborty, M. J. Ryan, D. Saha, M. H. Ahamed, S. Moyeen, S. K. Das, M. F. Ali, M. R. Islam, et al., "A comprehensive review of available battery datasets, rul prediction approaches, and advanced battery management," *Ieee Access*, 2021.
- [10] L. Wang, Y. Y. Tan, and X. L. Cui, "The application of labview in data acquisition system of solar absorption refrigerator," in *Advanced Materials Research*, vol. 532, pp. 581–585, *Trans Tech Publ*, 2012.
- [11] S. Hochreiter and J. Schmidhuber, "Long short-term memory," *Neural computation*, vol. 9, no. 8, pp. 1735–1780, 1997.
- [12] T.-H. Wu, J.-K. Wang, C.-S. Moo, and A. Kawamura, "State-of-charge and state-of-health estimating method for lithium-ion batteries," in *2016 IEEE 17th Workshop on Control and Modeling for Power Electronics (COMPEL)*, pp. 1–6, *IEEE*, 2016
- [13] F. Yang, S. Zhang, W. Li, and Q. Miao, "State-of-charge estimation of lithiumion batteries using lstm and ukf," *Energy*, vol. 201, p. 117664, 2020.
- [14] S. Santhanagopalan and R. E. White, "Online estimation of the state of charge of a lithium ion cell," *Journal of power sources*, vol. 161, no. 2, pp. 1346–1355, 2006.
- [15] B. Chinomona, C. Chung, L.-K. Chang, W.-C. Su, and M.-C. Tsai, "Long short-term memory approach to estimate battery remaining useful life using partial data," *IEEE Access*, vol. 8, pp. 165419–165431, 2020.